

Elaboration of Doped and Composite Nano-TiO₂

R. Azouani, S. Tieng, A. Michau, K. Hassouni, K. Chhor, J.-F. Bocquet, J.-L. Vignes,
A. Kanaev*

Laboratoire d'Ingénierie des Matriaux et des Hautes Pressions, UPR1311 C.N.R.S., Institut
Galilée, Université Paris-Nord, 93420 Villetaneuse, France

Turbulent mixing of reactive fluids in sol-gel process allows elaboration of monodispersed pure, doped and composite TiO₂ nanoparticles and nanocoatings on their base. In this work, we investigate the effect of hydroxyurea on the growth kinetic of TiO₂ nanoparticles and photocatalytic activity of the prepared N-TiO₂ nanocoatings in the visible. The materials was characterized by XRD, ATD, and XPS methods. Particular attention was given to their thermal treatment. Composite Ag(Au)-TiO₂ nanocoatings were also prepared by surface reduction induced by the UV-A illumination of amorphous TiO₂ nanoparticles.

I. Introduction

Since the discovery of Fujishima et al. (1972) of the photo-induced decomposition of water on titanium dioxide (TiO₂) electrodes, semiconductor-based photocatalysis has attracted extensive interest. In particular, TiO₂ became widely used material in heterogeneous photocatalysis for the destruction of highly toxic molecules and remediation of pollutants. It is inexpensive, nontoxic, resistant to photo-corrosion, and has high oxidative power. A relative drawback of this photocatalyst is related to its rather large band-gap that enables absorption of light of the UV-A spectral range. In particular, two most important polymorphs of TiO₂ anatase and rutile respectively absorb below 390 nm (band gap energy $E_g=3.2$ eV) and 413 nm ($E_g=3.0$ eV). This fundamental absorption covers only a minor part of 3-5% of the solar radiation. The challenge is to produce new generation photocatalysts with the extended photocatalytic activity to the visible spectral region ($\lambda>400$ nm). This requires a red shift of the absorption onset. A great deal of the related research has been focused on TiO₂ doping with both transition metal and non-metal impurities. More recently, particular concern has been given to the anionic doping of TiO₂ theoretically inspected by Asahi et al. (2001).

The visible-light photocatalytic activity of nitrogen-doped TiO₂ materials was reported for the first time by Sato (1986). A considerable progress in synthesis and understanding of this doped catalyst performance has been achieved last decade. Several research groups reported the visible-light activity of new N-doped TiO₂ materials prepared by different methods and using different nitrogen sources (e.g. Gandhe et al., 2005; Ihara et al. 2003, Li et al., 2005; Di Valentin et al., 2007). Doping seems to induce the band-gap narrowing at high N-loadings. However, most of results were obtained with relatively low loadings (~1%), which induce isolated sub-band impurity

* Correspondent author. E-mail: kanaev, azouani@limhp.univ-paris13.fr

levels close to the valence band. Moreover, oxygen vacancies may play an important role (Serpone, 2006).

Two important problems related to these material elaboration are (i) homogeneous repartition of a dopant over the host matrix and (ii) dopant retention at the calcinations process, which renders the material crystalline or improves the crystallinity. In this work, we present an original method of the elaboration of homogeneously N-doped TiO_2 nanocoatings by sol-gel process. We use hydroxyurea as dopant and add it at the nucleation stage, where reactive TiO_2 clusters and nanoparticles are created. This leads to an excellent material homogeneity, at least on the size-scale of the generated TiO_2 units (2-5 nm). Photocatalytic test using trichloroethylene (TCE) shows an increased activity of the elaborated nanocoatings under the visible light illumination.

II. Experimental details

II.1 Elaborations of nitrogen doped nanoparticles

The nanoparticles are synthesized in a sol-gel reactor with turbulent mixing of two reactive fluids containing titanium tetraisopropoxide (TTIP) of 98% purity (Interchim) and distilled water in 2-propanol. This device was described in details by Rivallin et al. (2005). Its main part is the T-mixer operating at high Reynolds numbers $\text{Re} \geq 4.4 \cdot 10^3$. The particle size and polydispersity significantly decrease in these conditions, corresponding to the Kolmogorov length smaller than $3 \mu\text{m}$ (Azouani et al., 2008). This reactor assures reproducibility of fast process kinetics and allows generation of TiO_2 nuclei ($2R=5.2 \text{ nm}$) and sub-nucleus units - clusters of size 2.0 nm and 3.2 nm (Azouani et al., 2007). The N-doped TiO_2 nanoparticles and clusters were obtained by an injection of hydroxyurea (HyU) in the reaction zone at the mixing stage. We conducted the process at the reactor bath temperature of 20°C , molar TTIP concentration $C_{\text{Ti}}=0.146 \text{ M}$ and hydrolysis ratio $H=C_w/C_{\text{Ti}}=2.0$. We have prepared several prestina (S0) and N-doped (S1-S8) TiO_2 samples presented in Table 1.

Table 1: Details of prepared N-doped TiO_2 samples.

Sample	S0	S1	S2	S3	S4	S5	S6	S7	S8
HyU, M	0	0,004	0,0053	0,0067	0,008	0,009	0,010	0,012	0,013

II.2 Influence of nitrogen on the Kinetic of nanoparticle of TiO_2

Particle size ($2R$) and total scattered-light intensity (I) by the particles population were continuously monitored by 1-minute samplings series using monomode optical fiber probe and He-Ne laser as a coherent light source by the photon-correlated spectroscopy method. The data were proceeded by 16-bit/255-channel PC board plugged digital correlator (PhotoCor Instruments) developed by Yudin et al. (1997).

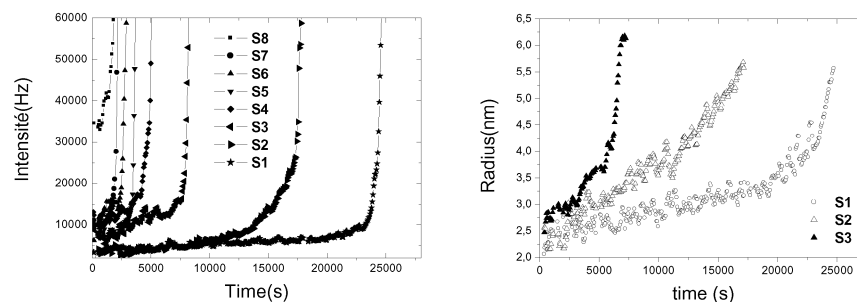


Figure 1: Scattered light intensity and size dependence on time for different N-doping ($H=2$).

The kinetics measurements of (I,R) were performed during the preparation for each of the samples S0-S8 and shown in figure 1. Both indicate the induction period, characteristic of the sol-gel process, at the end of which a precipitate is formed of large μm -size particles. However according to Azouani et al. (2007), the induction time tends to infinity in the preparation conditions and the formed 5.2-nm nuclei are metastable. The fastening of the induction kinetics therefore evidences reactions between HyU and TiO_2 nuclei resulting in the N incorporation into their body. The evolution of the radius confirms the influence of the dopant on the process kinetic. We remark that the initial curves slopes of the considered samples correlate to the induction time. This apparently indicates that the underlying kinetics mechanism is similar to that earlier proposed for the pure reactive TiO_2 colloids (Rivallin et al., 2005).

The prepared nanoparticles are yellowish and exhibit a strong visible absorption below 550 nm. Complementary optical absorption measurements have shown that the doping reactions are complete with no signs of saturation even at highest dopant loadings.

II.3 Thermal treatment of N-doped TiO_2

The preparation of the N-doped TiO_2 catalyst passes by the stage of the thermal treatment. In order to observe an influence of this stage, the precipitate of the reactive colloid S8 with highest N-content was dried (80°C for hours) and calcinated at different temperatures between 350 and 700°C during 4 hours. The powder X-ray diffraction (XRD) patterns obtained using INEL XRG-3000 device are shown in figure 2. They indicate the appearance of the anatase polymorph characteristic of pure TiO_2 at temperatures $\geq 350^\circ\text{C}$, while the rutile polymorph progressively sets up at $T \geq 700^\circ\text{C}$.

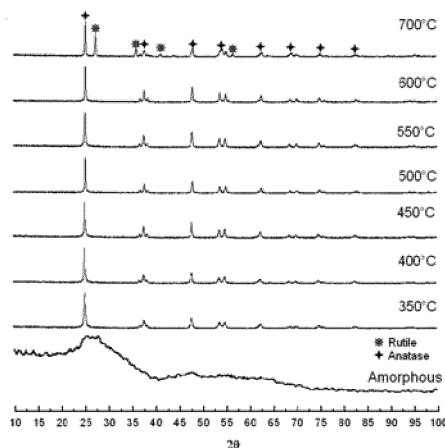


Figure 2: XRD patterns of N-doped TiO_2 .

Differential thermal analysis (DTA) shown in figure 3 was done using SETARAM TG92 Thermoanalyser on three samples: pure TiO_2 and N-doped TiO_2 samples S1 and S4 (see table 1). It confirms the general picture, characterised by two strong lower-temperature endothermic (125°C) and higher temperature exothermic (400°C) peaks that correspond to the principal mass loss domain. The first is due to the solvent (2-propanol) desorption whereas the second indicates the anatase crystalline phase appearance. The minor exothermal peak at 600 - 700°C is not accompanied by a mass loss and is due to the anatase-to-rutile phase transformation. Less prominent endothermal peaks at 250°C (not existed in the pure S0 sample and related to a mass

loss in S1/S4 samples) may belong to a partial desorption of HyU from the nano-TiO₂ surface.

The most interesting effect is the shift of the exothermic peak correspondent to the anatase formation to higher temperatures: from 407°C in pure TiO₂ to 415°C (S1) and 416°C (S4) in the N-doped TiO₂. The anatase-to-rutile phase transformation seems also to shift to higher temperatures in the N-doped TiO₂. This fact may indicate the stabilization effect induced by the doping.

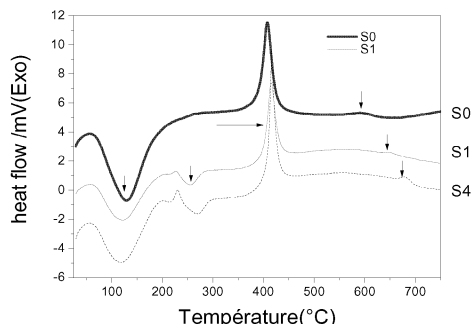


Figure 3: DTA patterns of pure and doped TiO₂.

X-ray photoelectron spectroscopy (XPS) was used to evaluate the amount and binding of nitrogen atoms in the N-doped TiO₂ powders before and after calcinations (table 2). While the O/Ti ratio is close to the expected stoichiometry, the N/Ti ratio significantly decreases after calcinations (we remark that in the amorphous sample the N/Ti ratio corresponds to the total amount of added HyU that confirms its reactions with TiO₂ nanoparticles). An apparent instability of this last value in S6 and S8 samples indicates extreme sensibility of the N-retention process to temperature fluctuations. We remark that N1s shows up in very weak 398 eV (N1), major 400 eV (N2) and weaker 401.5 eV (N3) peaks. According to Ashai et al. (2007), N1 and N2 may belong in our case respectively to substitutional NO_o and interstitial NO_i sites. The higher energy peak N3 showed no sensitivity to HyU addition (samples S1-S8) and can therefore be attributed to external nitrogen impurities adsorbed at the extended interface of nano-TiO₂ (~450 m²/g). Theoretical analysis by Di Valentin et al. (2007) affirms dominant interstitial nitrogen species in our preparation conditions.

Table 2: Atomic ratios of oxygen, nitrogen and carbon reported to titanium.

Samples	Thermal treatment	O/Ti ^{a)}	N/Ti ^{a)}	C/Ti ^{a)}
S0 (pure TiO ₂)	Yes	2.12	0.015	0.77
S8	No, amorphous	2.37	0.149	1.71
S6	Yes	2.27	0.073	0.93
S8	Yes	2.16	0.013	0.73

^{a)} XPS results are presented by P. Eloy and E. M. Gaigneau (Université Catholique de Louvain).

II.4 Photocatalytic activity of pure and doped nanocoatings

The N-TiO₂ doped catalyst was prepared by setting 1-mm glass beads in a contact with the reactive colloids for a short time, followed by their withdrawal into a dry atmosphere, drying at 80°C for several hours and calcinations at temperatures T=350, 400, 450 or 500°C during 4 hours. We used in the current experiments TiO₂ clusters/nanoparticles prepared with different hydrolysis ratios of H=1.25 (size 2.0 nm), 1.6 (3.2 nm) and 2.2 (5.2 nm) and maximum HyU addition correspondent to S8 sample.

The photocatalytic activity of the prepared N-material under visible light illumination was checked in a fixed bed reactor using trichloroethylene (TCE) as the model pollutant. This installation was previously described by Benmami et al. (2005; 2006) for the UV test. In the current experiments we installed 8-W UV-visible lamps (10% photons at $\lambda \leq 400$ nm) with maximum spectral intensity at 500 nm.

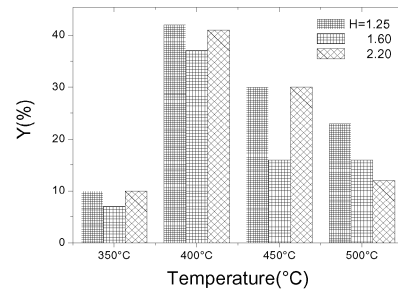


Figure 4: Photocatalytic activity of the N-doped TiO_2 in the visible spectral range.

Figure 4 shows the photocatalytic yield ($Y=1-\text{TCE}_{\text{in}}/\text{TCE}_{\text{out}}$) of the prepared N- TiO_2 nanocoatings at different (T,H). Most strongly the samples activity depends on T: the maximum was obtained $T=400^\circ\text{C}$ for all H at. The decrease to lower and higher temperatures is explained respectively by losses of nitrogen and poor sample crystallinity. Another factor can be the specific surface of the nanostructured N- TiO_2 , which is expected to decrease at calcinations.

II.5 Nano- TiO_2 doped by silver and gold nanoparticles

The photocatalytic activity of the amorphous TiO_2 nanoparticles is an important experimental fact (Benmami et al., 2006) that permits composite nanostructured coatings (Zolotavin et al., 2008). In particular, nanometric silver and gold clusters were grown onto nano- TiO_2 by surface ions reduction induced by the UV-A illumination. In our experiments a monolayer of amorphous 5-nm TiO_2 nanoparticles were deposited on glass plate. This substrate was immersed in the 0.1 mM aqueous solution of AgNO_3 . At 355-nm laser irradiation with power density of ~ 10 mW/cm^2 , a characteristic gray color of the metallic silver appeared in the irradiated spot after few tens of seconds.

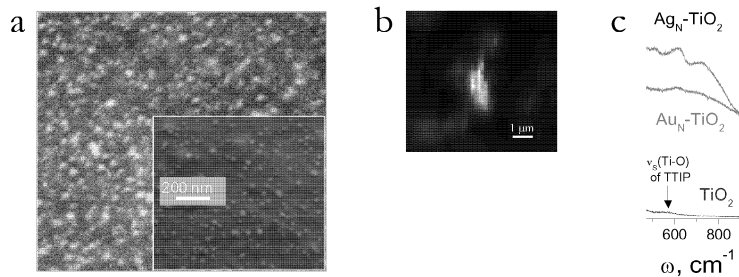


Figure 5: SEM image of composite $\text{Ag}_N\text{-TiO}_2$ nanocoating (a), its fluorescence image (Zolotavin et al., 2008) (b) and Raman spectra of different prepared nanocoatings (c).

A SEM (LEO S360) image of the composite nanocoating after a prolonged UV-A lamp irradiation (362 nm, $3\text{J}/\text{cm}^2$) is shown in figure 5a. It shows a homogenous surface recovery by silver nanoparticles of a mean size of 15 nm. A successful preparation of

the composite Au_N-nanoTiO₂ nanocoating was also achieved using gold reduction from AuCl₃. The surface plasmon enhancement was observed in both fluorescence and Raman spectra (figure 5b-c).

III. Conclusion

A control of the nucleation-growth stage in the sol-gel process permits preparation of finest metastable TiO₂ clusters and nanoparticles of 2R=2.0 nm, 3.2 nm, and 5.2 nm, which are suitable for the reactive doping. Hydroxyurea could be conveniently utilized to form N-TiO₂ nanoparticles in order to deposit them as nanocoatings. Our kinetic studies show that the reactivity of the doped nanoparticles considerably increases. XRD analysis shows that the catalyst was pure anatase at thermal treatment below 700°C. The DTA analysis indicates that nitrogen doping shifts the phase transformation anatase→rutile to higher temperatures. The XPS analysis evidences the incorporation of nitrogen in the interstitial sites, which efficiency sensibly depends on the treatment temperature. The photocatalytic activity under visible light illumination attains maximum for the materials calcinated at 400°C. Nanometric silver and gold clusters were grown onto amorphous TiO₂ nanoparticles by surface reduction induced by the UV-A illumination.

This work is supported by French network C'Nano (IdF) and COST D41 Action of the European Commission.

References

- Asahi R., Morikawa T., Ohwaki T., Aoki K., Taga Y., 2001, *Science* 293, 269.
- Asahi R., Morikawa T., 2007, *Chem. Phys.* 339, 57.
- Azouani R., Soloviev A., Benmami M., Chhor K., Bocquet J.-F., Kanaev A., 2007, *J. Phys. Chem. C* 111, 16243.
- Azouani R., Michau A., Hassouni K., Chhor K., Bocquet J.-F., Vignes J.-L., Kanaev A., 2008, *Proceedings of ISIC-17*.
- Benmami M., Chhor K., Kanaev A., 2005, *J. Phys. Chem. B* 109, 19766.
- Benmami M., Chhor K., Kanaev A., 2006, *Chem. Phys. Lett.* 422, 552.
- Di Valentin C., Finazzi E., Pacchioni G., Selloni A., Livraghi S., Paganini M.C., Giamello E., 2007, *Chem. Phys.* 339 44.
- Gandhe A.R., Fernandes J.B., 2005, *J. Solid State Chem.* 178, 2953.
- Li D., Haneda H., Shunichi H., Naoki O., 2005, *Mater. Sci. Engineer. B* 117, 67.
- Fujishima A., Honda K., 1972, *Nature* 238, 37.
- Ihara M.M., Iriyama Y., Matsumoto O., Sugihar S., 2003, *Appl. Catal. B* 42, 403.
- Pucher P., Benmami M., Azoauni R., Krammer G., Chhor K., Bocquet J.-F., Kanaev A. V., 2007, *J. Appl. Catal. A* 332, 297.
- Rivallin M., Benmami M., Kanaev A., Gaunand A., 2005, *Chem. Eng. Res. & Design*, 83(A1) 1.
- Rivallin M., Benmami M., Gaunand A. Kanaev A., 2004, *Chem. Phys. Lett.* 398, 157.
- Sato S., 1986, *Chem. Phys. Lett.* 123, 126.
- Serpone N., 2006, *J. Phys. Chem. B* 110, 24287.
- Yudin I.K., Nilolaenko G.L., Kosov V.I., Agayan V.A., Anisimov M.A., Sengers J.V., 1997, *Int. J. Thermophys.* 15, 1237.
- Zolotavin P., Permenova E., Sarkisov O., Nadtochenko V., Chhor K., Azouani R., Kanaev A., 2008, *Chem. Phys. Lett.* 457, 342.